Study of the $^{10}B(^{16}O, \alpha)^{22}Na$ reaction

J. Gomez del Campo,* J. L. C. Ford, Jr., R. L. Robinson, and P. H. Stelson

Oak Ridge National Laboratory,† Oak Ridge, Tennessee 37830

S. T. Thornton‡

University of Virginia, Charlottesville, Virginia 22901

(Received 2 July 1973)

States in ^{22}Na were populated using the $^{10}B(^{16}O, \alpha)$ reaction. Excitation functions were measured in the energy range $E_{c.m.} = 15.4 - 17.7$ MeV for 47 excited states in ^{22}Na from 0 to 14 MeV excitation. Angular distributions were measured at a bombarding energy of 46 MeV for a number of the excited states and were observed to be symmetrical around 90° (c.m.). Fluctuation analyses of the excitation functions were made, and the results indicated a statistical compound-nucleus process for the reaction mechanism. Hauser-Feshbach calculations gave good agreement with the data and provided strong evidence for proposed high-spin members of the ground-state rotational band, and the $K = 0^+$, $T = 0$ band in ^{22}Na.

$$\left[\begin{array}{l} \text{NUCLEAR REACTIONS } {}^{10}B({}^{16}O, \alpha), \; E_{16O} = 40 \text{ to } 46 \text{ MeV, measured } \sigma(E) \text{ for} \\ \theta_{lab} = 7°; \; E_{16O} = 46 \text{ MeV, measured } \sigma(\theta); \; {}^{22}Na \text{ deduced levels. Fluctuation analy-} \\ \text{sis. Hauser-Feshbach calculations and suggested } J \text{ values. Enriched targets.} \end{array} \right]$$

I. INTRODUCTION

Among the interesting features of heavy-ion reactions, the strong selectivity observed in the population of states in the residual nuclei,[1] usually of high spin,[2] has led to possible new forms of spectroscopy inaccessible to light-ion reactions. This selectivity of high-spin states is a feature of heavy-ion reactions due to the high angular momentum available.

As is well known, there has been much speculation about the different reaction mechanisms involved. Supporting evidence for a direct or semi-direct mechanism has been reported for the ^{12}C-(^{12}C, $\alpha)^{20}Ne$ reaction[3] populating two of the $K = 0^+$ bands. On the other hand since the early studies of these reactions,[4-7] strong evidence has been presented for a statistical compound-nucleus reaction description, particularly for the low-lying states. The recent report of Greenwood *et al.*[8] dealing with the $^{12}C(^{16}O, \alpha)$ reaction gives a good example of the compound-nucleus statistical mode of decay and shows the usefulness of Hauser-Feshbach calculations in describing such data. Another example of such calculations has been given for the energy-averaged angular distributions of the $^{12}C(^{16}O, \alpha)$ reaction.[9]

The level properties of the low-lying states in ^{22}Na have been investigated successfully by means of γ-ray decay studies,[10] lifetime measurements,[11] and one-[12,13] and two-nucleon[14] transfer reactions. Some studies of the states of ^{22}Na have been made by means of heavy-ion reactions[15-17] using the

$^{12}C + ^{14}N$ entrance channel, and suggestions[15,16] have been made for some of the high-spin members of the $K = 3^+$, $T = 0; K = 0^+$, $T = 0$; and $K = 1^-$, $T = 0$ rotational bands. None of these experiments present energy-averaged spectra, and consequently the observations are subject to the strong and rapid fluctuations with energy typical of heavy-ion reactions.

In the present study we have measured excitation functions for the $^{10}B(^{16}O, \alpha)^{22}Na$ reaction in order to average over a wide range of bombarding energies and to compare our results with fluctuation analyses and Hauser-Feshbach calculations. In addition we have measured angular distributions in order to detect possible asymmetries around 90° (c.m.). Data for the competing $(^{16}O, d)$ and $(^{16}O, {}^6Li)$ reactions were also measured to complete the Hauser-Feshbach analysis and are discussed elsewhere.[18]

A comparison of our data with Hauser-Feshbach calculations and shell-model predictions[19] allows us to suggest strong candidates for the high-spin members of the ground-state rotational band and the $K = 0^+$, $T = 0$ band.

II. EXPERIMENTAL PROCEDURE

Self-supporting, 95% enriched, ^{10}B foils with thicknesses ranging between 10-30 $\mu g/cm^2$ were bombarded with ^{16}O ions from the Oak Ridge tandem accelerator. The target thicknesses were measured by elastic scattering of 24-MeV $^{16}O^{4+}$ ions at a laboratory angle of 7°. The 4^+, 5^+, 6^+, 7^+, and 8^+ charge states of the scattered ^{16}O ions

were detected in a magnetic spectrometer, and a Rutherford scattering cross section was assumed. A second method of measuring the target thicknesses was also used, namely, by ranging the foils with a calibrated ^{241}Am α source. A typical target thickness was 17 μg/cm^2, and agreement within 10% was found between the two methods of determining the thickness.

The reaction products were detected at the focal plane of an Enge split-pole magnetic spectrograph by means of a 60-cm-long position-sensitive proportional detector of the Borkowski and Kopp type.[20,21] A more detailed description of the detector and electronics is given elsewhere.[18] An aluminum foil 7 mg/cm^2 thick was placed in front of the detector at forward angles to avoid the elastic ^{16}O peak during the (^{16}O, α) measurements. The data were recorded in 1024 channels of a multichannel analyzer and dumped onto magnetic tapes for analysis. The peaks of the (^{16}O, α) spectra were stripped with the aid of a light-pen system interfaced to a PDP-11 computer.

Since carbon buildup during bombardment can be a severe problem due to the large ^{12}C(^{16}O, α) cross section, it was minimized by cold trapping on the entrance beam line and between the scattering chamber and the diffusion pump. In some cases it was necessary to correct our spectra for α particles from the ^{12}C(^{16}O, α) reaction, which was possible as each ^{10}B(^{16}O, α) run was followed by a ^{12}C(^{16}O, α) run under the same conditions.

III. RESULTS

Excitation functions have been measured for many of the different states populated by the ^{10}B(^{16}O, α)-

^{22}Na reaction. An interval of bombarding energy from 40 to 46 MeV was covered in 200-keV steps at a laboratory angle of 7°. Figure 1 shows a typical spectrum taken at a laboratory energy of 44 MeV and angle of 7°. The experimental resolution [full width at half maximum (FWHM)] is of the order of 100 keV and is limited by the target thickness. The wide range of excitation energies (E_x = 0 to 14 MeV in ^{22}Na) which can be observed simultaneously with the detector is evident. The strong structure observed, as well as the selectivity of the reaction, indicates probable population of high-spin states. In this 14-MeV interval of excitation energy we have been able to analyze 47 states. Also shown in Fig. 1 are the known members of the ground-state rotational band with respective spin and energies (MeV) of 3$^+$ (0.0), 4$^+$ (0.89), and 5$^+$ (1.53), and the suggested 6$^+$ (3.71).[16,17] 7$^+$ (4.52),[15,16] and 8$^+$ (8.60)[15] members. In the present paper we give evidence that the 8.6-, 9.8-, and 13.6-MeV levels shown are probably the 8$^+$, 9$^+$, and 10$^+$ members of the ground-state rotational band.

In order to follow the shift with bombarding energy and angle of the different α-particle groups, a computer program was used to calculate the expected peak channel positions as a function of the excitation energy in the residual nuclei for a particular choice of reaction, bombarding energy, angle, magnetic field setting, and focal-plane setting after making a careful calibration of the detector and electronics by stepping α-particle groups from a ^{244}Cm source along the detector. Values so determined for the level energies of the known state generally agreed within 25 keV with the
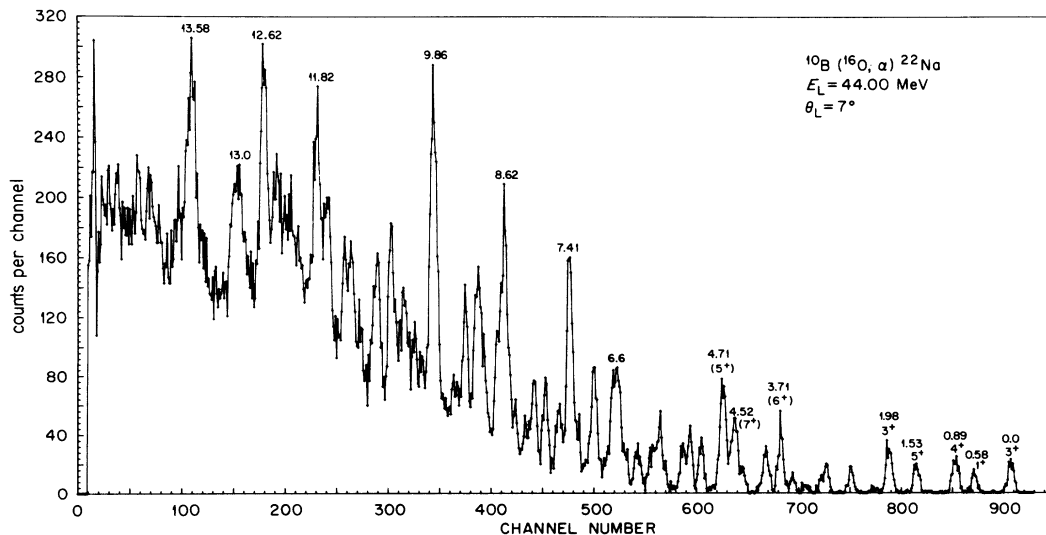

FIG. 1. A typical ^{10}B(^{16}O,α)^{22}Na spectrum measured at a bombarding energy of 44 MeV and a laboratory angle of 7°.

TABLE I. Cross sections for the $^{10}B + ^{16}O \to \alpha + ^{22}Na$ reaction at 10° (c.m.).

E_x [a] (MeV)	J^π	K^π	$\langle d\sigma(10°)/d\Omega\rangle_{exp}$ (mb/sr)	$\langle d\sigma(10°)/d\Omega\rangle_{H.F.}$ (mb/sr)	Γ_M (keV)	Γ_A (keV)
0.0	3+ [a]	3+ [a]	0.091	0.163	88.8	70.8
0.583	1+ [a]	0+ [a]	0.082	0.050	98.7	315.6
0.891	4+ [a]	3+ [a]	0.104	0.200	111.1	169.2
1.528	5+ [a]	3+ [a]	0.102	0.355	111.1	217.2
1.937	1+ [a]	0+ [a]				
1.952	2+, T=1 [a]	0+ [a]	{0.168			
1.984	3+ [a]	0+ [a]		0.125	98.7	290.4
2.211	1− [a]	1− [a]	0.019	0.015	111.1	154.8
2.572	2− [a]	1− [a]	0.051	0.055	98.7	50.4
2.969	3+ [a]		0.055	0.100	111.1	175.2
3.059	2+ [a]	(1+) [a]	0.046	0.050	111.1	120.0
3.521	3− [a]	1− [a]	0.053	0.080	111.1	271.2
3.708	(6+) [a]	(3+)	0.108	0.300	148.1	283.2
3.944	1+ [a]	(1+) [a]	0.060	0.030	98.7	63.6
4.466	(4−) [b]	(1−) [b]	0.053	0.120	98.7	56.4
4.522	(7+) [b]	(3+) [b]	0.253	0.450	111.1	218.4
4.708	(5+) [b]	(0+) [b]	0.258	0.245	126.9	648.0
4.720	0+ → 4+					
5.117	(4+) [c]		{0.138	0.110	111.1	56.4
5.165						
5.317	1+,2+,3+,4+ [c,a]		0.208	0.110	148.1	135.6
5.44	3− [c] (0−,1−,2−) [a]		0.082	0.063	126.9	231.6
5.605	1+,2+ [a]					
5.83	(5+) [c]		{0.21	0.20	98.7	80.4
5.858						
5.938			{0.117			
5.953					111.1	80.4
5.995						
6.185	0+ → 4+ [a]		{0.116			
6.247	(5−) [c]			0.125	98.7	80.4
6.557	1+,2+ [a]		{0.391			
6.582	(6+) [c]			0.21	111.1	80.4
7.008	(0+,1+,2+,3+,4+) [a]		{0.273			
7.081					88.85	294.0
7.367			{0.444			
7.413	(6−) [c]			0.275	98.7	96.0
7.595			{0.267			
7.633					111.1	340.8
7.884			{0.257		111.1	64.8
7.942						
7.963			{0.158			
8.026					98.7	190.8
8.157			{0.155			
8.198					98.7	91.2
8.367			{0.121			
8.417					98.7	90.0
8.602	(8+) [b,c,d]	(3+) [b,d]	0.49	0.30	88.8	45.6
8.674			0.11		98.7	50.0
9.008			{0.575			
9.051	(7+) [c,d]	(0+) [d]		0.305	98.7	206.0
9.312	(7+) [c,d]		{0.403	0.300	98.7	112.8
9.360						
9.527			{0.152		111.1	112.8
9.582						
9.859	(9+) [c,d]	(3+) [d]	{0.611	0.47	126.9	274.8
9.908						
10.4 [e]			0.267		111.1	58.8
10.61 [e]	(7−) [c]		0.367	0.220	98.7	69.6

TABLE I (Continued)

E_x [a] (MeV)	J^π	K^π	$\langle d\sigma(10°)/d\Omega\rangle_{exp}$ (mb/sr)	$\langle d\sigma(10°)/d\Omega\rangle_{H.F.}$ (mb/sr)	Γ_M (keV)	Γ_A (keV)
10.87 [e]			0.331		98.7	45.0
11.20 [e]			0.333		88.8	45.0
11.39 [e]			0.266		98.7	82.8
11.66 [e]			0.320		111.1	45.0
11.82 [e]	(8$^-$) [c]		0.442	0.280	111.1	78.0
12.46 [e]			0.355		111.1	73.0
12.62 [e]	(9$^+$) [c,d]	(0$^+$) [d]	0.450	0.350	98.7	42.0
12.87 [e]			0.325		98.7	52.0
13.01 [e]			0.320		111.1	53.0
13.58 [e]	(10$^+$) [c,d]	(3$^+$) [d]	0.478	0.260	111.1	85.2
13.75 [e]			0.239		111.1	60.0

[a] References 12–14.

[b] Reference 15.

[c] Spin included in the Hauser-Feshbach calculation (see discussion in text).

[d] Suggested by the present experiment.

[e] Excitation energies from the present experiment.

values reported in Refs. 12–14, a difference well within our experimental resolution of about 100 keV.

Table I summarizes our results for the different α-particle groups. The excitation energies of column 1 are those of Garrett $et\,al.$[12-14] up through 9.908 MeV. Above 10 MeV our measured excitation energies are given in the table. The differential cross sections averaged over the interval 40–46 MeV from the measurements at 7° (lab) are listed in column 4. The uncertainty in the absolute cross sections varies from about ±15% to ±25%. In column 5 of Table I we present the results of the Hauser-Feshbach calculations for the differential cross sections for some of the levels studied which will be discussed in Sec. V. The coherence widths which were calculated by the method of counting maxima, as well as by autocorrelation-coefficient measurements are listed in columns 6 and 7, respectively, and a further discussion of these widths is presented in Sec. IV. The spins and parities of the known states in ^{22}Na, as well as the quantum numbers for the various rotational bands, are taken from Refs. 12–15 and are listed in columns 2 and 3, respectively, except for those states whose values are suggested in the present paper and which are distinguished by the footnote c.

Figure 2 shows the measured excitation functions for some of the more interesting states in ^{22}Na as a function of the incident energy in the center-of-mass system. Plotted on the left side of Fig. 2 are the known 3$^+$, 4$^+$, and 5$^+$ members of the ground-state rotational band ($K^\pi = 3^+$, $T = 0$) as well as the possible candidates for the 6$^+$ to 10$^+$ mem-
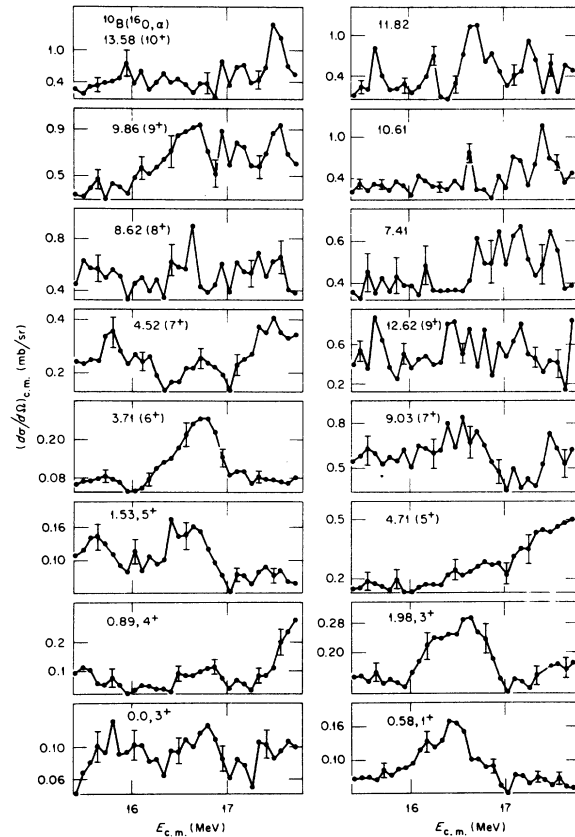

FIG. 2. Excitation functions for some of the excited states in ^{22}Na plotted as a function of the center-of-mass energy. Notice that the vertical scale is linear and displaced from zero.

bers to be discussed in Sec. V. On the right side of the figure are those known or suggested members for the $K^{\pi} = 0^{+}$, $T = 0$ band up to the 9^{+} state. The remaining excitation functions are for strongly excited states at 7.41, 10.61, and 11.82 MeV.

As can be seen from Fig. 2, we observed the typically strong and rapid fluctuation of the cross sections with energy from which the distribution about the average value can be analyzed using simple statistical theory.[4, 6-8] In a number of the excitation functions strong structure was observed in the general energy region between 16 and 17 MeV (c.m.). The fluctuation analysis discussed in Sec. IV also indicated a significant cross correlation between the excitation functions for some of the levels.

Angular distributions for many of the observed levels were measured at a laboratory energy of 46 MeV. In Fig. 3 we show a typical spectrum for the $^{10}B(^{16}O, \alpha)$ reaction for an energy of 46 MeV and a laboratory angle of 120° (~140° c.m.). The experimental resolution is of the order of 80 keV and much of the structure observed at forward angles is present. The various excited states are identified by the excitation energies of Table I. The length of the detector limits the region of excitation energy covered to a smaller interval than for the spectra at forward angles because of the strong shift in energy of the various α-particle groups with angle.

Figure 4 shows several of our measured angular distributions. The left side of Fig. 4 displays the known and suggested members of the ground-state rotational band up to the 10^{+} state, whereas the right side shows those observed for the $K^{\pi} = 0^{+}$,

$T = 0$ band up to the 9^{+} member. The remaining states shown at 9.31, 7.41, and 5.11 MeV are some of the states prominently excited.

The estimated error in the absolute cross sections shown in Fig. 4 varies from 20 to 35% depending on counting statistics, background subtraction, and target-thickness uncertainty. Of particular concern are the points at 90° lab (~110° c.m.) in which we assume a larger uncertainty because at this angle it was impossible to completely correct for the large kinematic shift by moving the focal-plane position. The data are clearly symmetric around an angle of 90° (c.m.) consistent with a compound-nucleus process. The curves drawn through the data points are the result of Hauser-Feshbach calculations discussed in Sec. V.

Although the observed angular distributions provide strong evidence for a compound-nuclear reaction mechanism, they were measured at a single energy and might be affected by fluctuation phenomena. However, Fig. 5 shows the angular distribution for the sum of the levels observed from 0.0 to 6.6 MeV, as well as for the sum from 0.0 to 10 MeV, although in this case data were only available at forward angles for the states above 6.6 MeV. Also shown, normalized to the data, is the function $1/\sin\theta$, which is the expected energy-averaged angular distribution for a statistical compound-nucleus model involving many large angular momenta.[22] It is interesting that the points for the sum over the larger region of excitation energy, including more high-spin states, show less fluctuation than those in the lower portion of the figure.
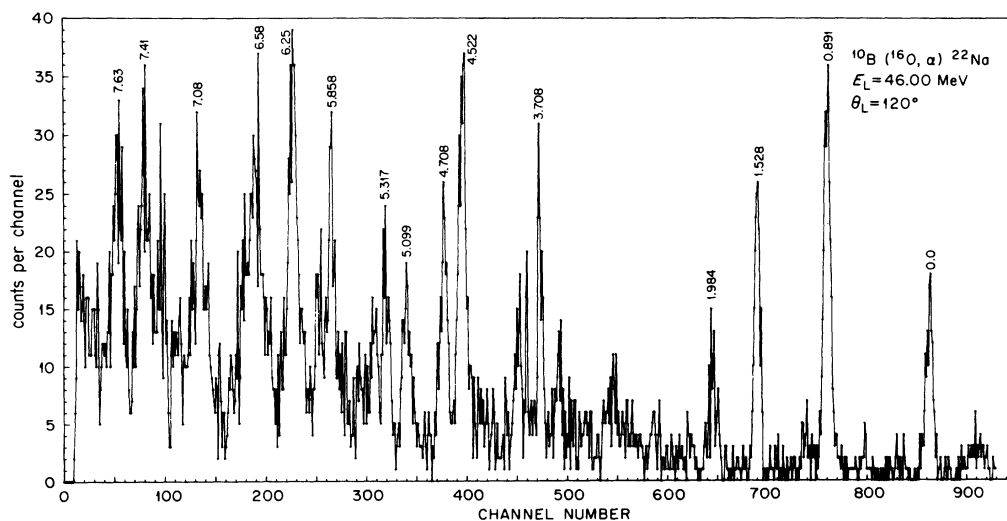

FIG. 3. A $^{10}B(^{16}O, \alpha)^{22}Na$ spectrum obtained at a bombarding energy of 46 MeV and a laboratory angle of 120°.

IV. FLUCTUATION ANALYSIS

Comparison of the excitation functions with fluctuation analysis can determine if the observed experimental fluctuations are compatible with a statistical description, and if so, can be used to extract the average properties of the participating compound states. Of particular importance is the measurement of the coherence width of the fluctuations which equals the average width Γ of the compound states.

The theoretical formulation of Ericson[23] and Brink and Stephen[24] was used to analyze our data, mainly because of the simplicity with which the various quantitative results can be extracted from the data. In particular, the comparison between predicted and measured probability distributions is useful to determine the possible direct contribution to the reactions as has been pointed out by

the work of Halbert, Durham, and van der Woude.[4] The predicted probability distribution for the ratio $x = \sigma/\langle\sigma\rangle$ has the form

$$P_N(x) = \left(\frac{N}{1 - y_D}\right)x^{N-1}\exp\left[\frac{-N(x + y_D)}{1 - y_D}\right]$$

$$\times \frac{J_{N-1}[2iN(xy_D)^{1/2}/(1 - y_D)]}{[iN(xy_D)^{1/2}/(1 - y_D)]}, \quad (1)$$

where J_{N-1} is the cylindrical Bessel function with imaginary argument, σ refers in our case to the measured center-of-mass differential cross section at the energy ϵ, and $\langle\sigma\rangle$ is the differential cross section averaged over the interval of bombarding energy. The quantity y_D is the ratio of σ_D, the direct component of the reaction cross section, to the total reaction cross section. The number of effective channels N contributing to the reaction is also known as the fluctuation damping coefficient.[25]

Our results for the probability distributions are presented in Fig. 6. The histograms, normalized
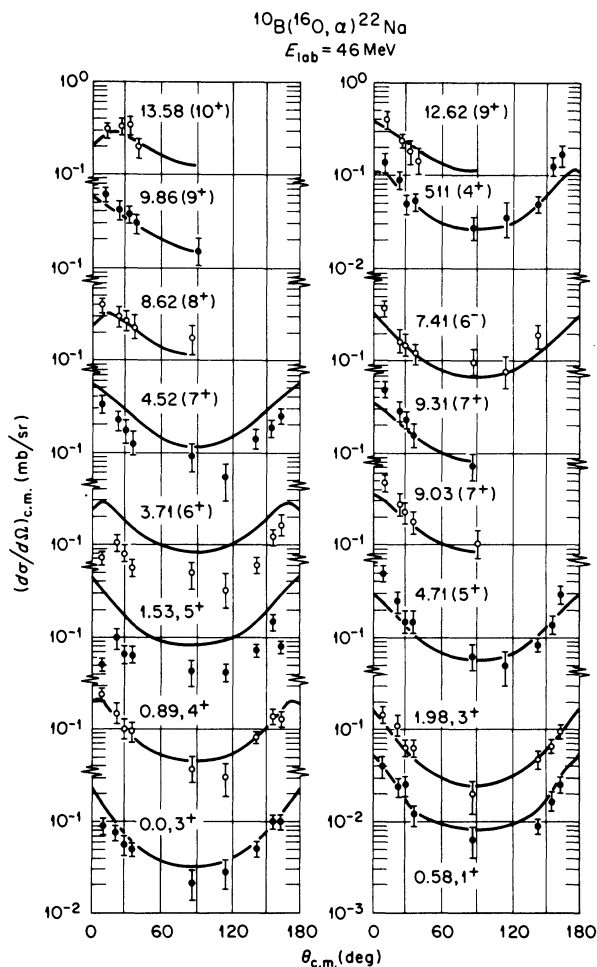

FIG. 4. Angular distributions for some of the excited states in ^{22}Na measured at a bombarding energy of 46 MeV. The solid lines are the result of Hauser-Feshbach calculations discussed in Sec. V in the text.
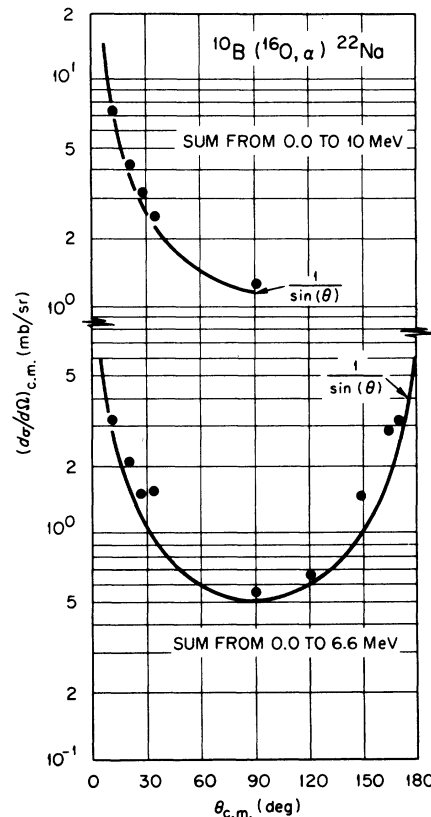

FIG. 5. A comparison between the sum of the angular distributions of the various α groups with a normalized $1/\sin\theta$ function; the limiting case predicted by the statistical model when many high angular momenta are involved.

to unit area determined from the experimental points, are compared with theoretical distributions $P_N(x)$ calculated under the assumption that the direct component is zero, i.e., $y_D = 0$. Adequate fits were obtained to most of the experimental histograms seen in Fig. 6. Exceptions are the 3^+ ground state, which is especially poorly fitted by either P_{10} or P_{20}, and in fact could not be fitted well by any combination of y_D and N, and the 3.718-MeV (6^+) state. The excitation function of the 3.718-MeV state shows a very broad and large peak at about 16.7 MeV, as well as severe damping of the fluctuations, causing an unusual probability distribution. Similar anomalies have been observed in previous analyses of other reactions (see, e.g. Ref. 4).

The extracted values for N, which are upper limits to the real number of effective channels, range from 6 to 25 for the levels studied. With some exceptions, there is a general tendency for N to increase with the spin of the final nucleus. The maximum value for N is expected to occur at $90°$ in the center-of-mass system. Assuming that all the different magnetic substate components of the cross section contribute equally, an approximation for the maximum value of N is $\frac{1}{2}[(2I+1)(2i+1) \times (2I'+1)(2i'+1)]$, where I and i are the spins in the entrance channel and I' and i' are those in the exit channel.[25] In the case of the $^{12}C(^{16}O, \alpha)$ reaction, the value of N near $\theta_{c.m.} = 10°$ has been estimated by Gibbs and Richter to be half the maximum value (see Ref. 8). Since the amounts of angular momenta involved in the present $^{10}B(^{16}O, \alpha)$ experiment and in the $^{12}C(^{16}O, \alpha)$ experiment of Greenwood *et al.*[8] are very similar, we used the same estimate to obtain expected values for N between 5 and 36 (for spin values of 1 through 10) in reasonable agreement with those obtained from the probability distributions which correspond to data measured at $10°$ (c.m.). One could determine equally good fits to the probability distributions for various choices of N and nonzero values of y_D. However, large y_D requires unreasonably small N values, and thus the distributions in Fig. 6 contain no convincing evidence for a direct contribution to the reaction process.

Another informative characteristic of the excitation functions for determining the possible presence of nonstatistical components to the reaction are the cross-section auto- and cross-correlation functions. In addition, the autocorrelation coefficients may determine the coherence widths Γ of the compound-nucleus states involved. Autocorrelations were determined by the relation

$$R(\epsilon) = \frac{\langle \sigma(E)\sigma(E+\epsilon)\rangle}{\langle \sigma(E)\rangle\langle \sigma(E+\epsilon)\rangle} - 1, \qquad (2)$$

where $\sigma(E)$ is the measured differential cross section at energy E, ϵ is the energy interval between data points, and from this we determine Γ, the average coherence width. Our extracted Γ values for all 47 states based on the usual procedure of fitting a Lorentzian to the measured autocorrelation function are shown in column 7 of Table I and are labeled Γ_A. These values have been corrected for the effects of energy resolution and finite sample size in the manner described by Halbert, Durham, and van der Woude.[4] Although the interval between data points was comparable to the extracted widths, these values should be at least an upper limit to Γ. The values fluctuate as might be expected from both the experimental conditions and a possible dependence on the spin and excitation energy of the state in question,[8,26] but are in reasonable agreement with values obtained by similar analyses in this mass region.[4,7,27] If one averages
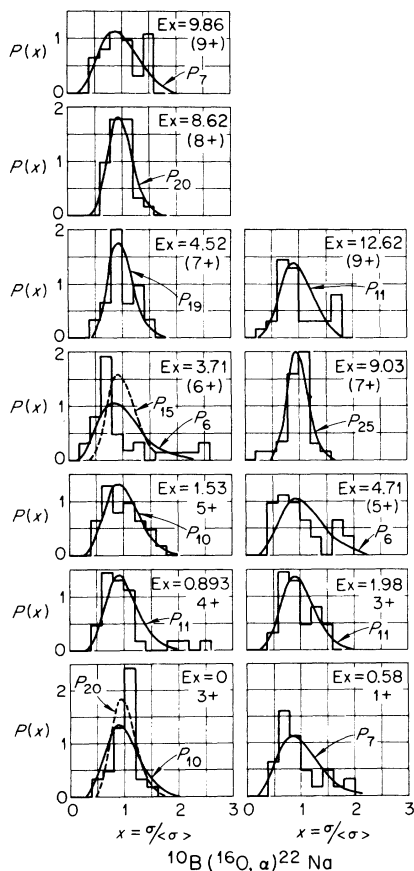
$^{10}B(^{16}O, \alpha)^{22}Na$

FIG. 6. The measured and calculated probability distributions. The histograms were obtained from the experimental excitation functions, and the solid curves are the statistical predictions obtained from Eq. (1) in the text calculated assuming a zero direct component.

over the observed Γ_A values to obtain an average width associated with the average participating compound-nuclear states, a value of 140 keV is obtained. However, individual values in Table I fluctuate widely around this average.

Another method of determining Γ is that of counting the number of maxima M in the interval I of the excitation function. The average width is then $\Gamma = Ib_N/2M$ and has been used in several analyses of cross sections (see, e.g. Ref. 4). The main uncertainties in this method come from the uncertainty in the number of maxima M and the value of the constant b_N which, however, includes the effects of finite energy steps. For our case in which $\epsilon = 77$ keV, the interval between data points in the center-of-mass system, and N equals about 10, we used a value of 0.77 for b_N obtained from Ref. 28 to determine the Γ_M values listed in column 6 of Table I. The average $\langle \Gamma_M \rangle$ is then 107 keV, again in reasonable agreement with systematics in this region of mass and excitation energy.[27] The difference between the values determined by the two techniques is also similar to that found in other studies (see, e.g. Ref. 4). However, the deviation of the individual Γ values about the average is a good deal smaller using the method of counting maxima, which in the present case should be the more reliable method of determining Γ.[4,28]

Possible cross correlations between the excitation functions for different excited states were investigated by the relationship[6, 25]

$$R_\epsilon(\alpha, \alpha') = \frac{\langle \sigma_\alpha(E)\sigma_{\alpha'}(E + \epsilon) \rangle}{\langle \sigma_\alpha(E)\rangle\langle\sigma_{\alpha'}(E + \epsilon) \rangle} - 1, \quad (3)$$

where ϵ stands for the energy interval concerned, and α and α' represent any two different levels populated. Figure 7 presents the measured cross correlation coefficients for $\epsilon = 0$ for all 47 levels studied, as well as for 18 levels which showed broad structure between 16 and 17 MeV (c.m.) in the excitation functions (see Fig. 2). According to the statistical model the different channels α, α' should be uncorrelated, meaning that the probability distributions should be symmetric Gaussians about the value $R_{\epsilon=0}(\alpha, \alpha') = 0$. The histogram at the top of Fig. 7 indicates essentially no correlation between the excitation functions as a whole. However, the bottom histogram indicates the presence of some correlations between the excitation functions which display broad structure.

The general comparison of the data with the fluctuation analyses is consistent with a compound-nuclear reaction mechanism. However, it is impossible to rule out the possibility of a small direct component. The fact that there is some correlated structure between center-of-mass energies of 16

and 17 MeV (especially for the levels at 0.58, 1.53, 1.98, and 3.71 MeV in Fig. 2) could be an indication of an entrance-channel effect. Such effects should also be seen in the elastic scattering at the same energies. However, they could also be described by a statistical means as intermediate resonances of the type discussed by Moldauer.[29]

V. HAUSER-FESHBACH CALCULATIONS

Since the observed symmetry of the angular distributions and the results of the fluctuation analyses suggest a predominantly compound-nucleus reaction mechanism for the present reaction, we decided that a Hauser-Feshbach analysis of the data was justified. Hauser-Feshbach calculations are complicated since a highly excited nucleus can decay through many energetically open channels, and the flux emitted in each exit chan-
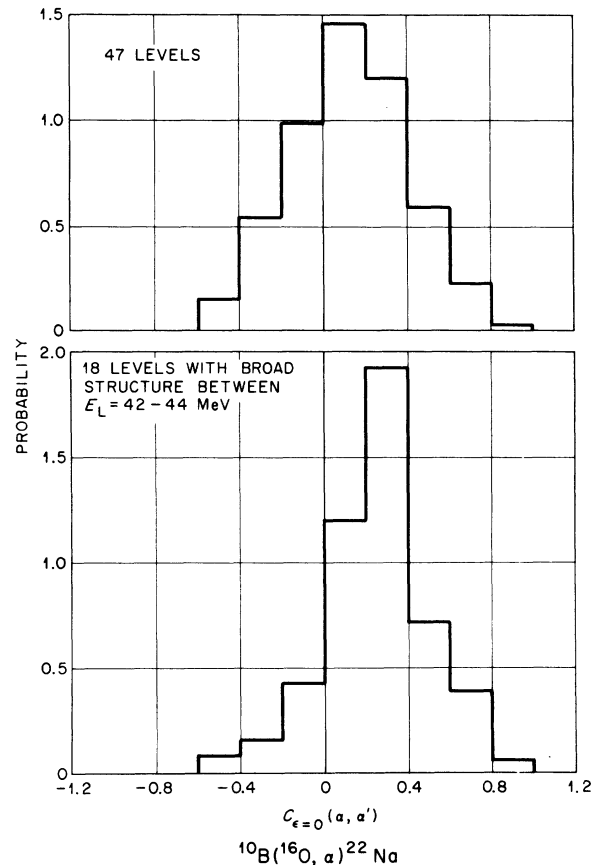

FIG. 7. Results of the cross correlation coefficient plotted as a probability distribution normalized by the factor $C_{\epsilon=0}(\alpha, \alpha') = R_{\epsilon=0}(\alpha, \alpha')/[R_{\epsilon=0}(\alpha) R_{\epsilon=0}(\alpha')]^{1/2}$. The top histogram was obtained from all 47 levels observed, and the bottom one includes only the 18 levels which indicated broad structure in the excitation functions between 16 and 17 MeV (c.m.).
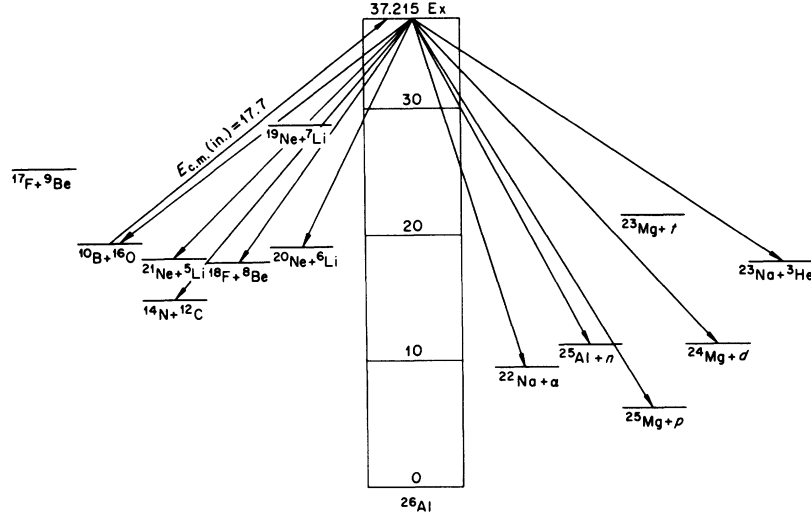
FIG. 8. The compound-nuclear system ^{26}Al and the channels energetically open to decay. The arrows coming out of the compound system represent the various channels included in the Hauser-Feshbach calculations.

nel depends on the angular momentum available and on the amount of excitation energy left in the final nucleus. For the ^{10}B + ^{16}O — ^{26}Al system the most important exit channels are presented in Fig. 8. At an incident energy of 17.7 MeV (c.m.) the compound nucleus ^{26}Al is formed with an excitation energy of 37.2 MeV, and primarily in high-spin states in part due to the large entrance-channel spin of 3^+. At this excitation energy there are many open channels for the decay and from energy considerations alone the most favored ones would be the p, n, d, and α channels. However one cannot exclude the contribution of the other channels particularly at low excitation energies of the final nuclei where angular momentum effects play the most important role. Fig. 9 shows a plot of the grazing angular momentum for the different channels α obtained from the semiclassical relation[30]

$$l_\alpha (l_\alpha + 1) = 2 M_\alpha R_\alpha^2 (\epsilon_\alpha - C_\alpha) \hbar^2 , \qquad (4)$$

where M_α is the reduced mass, R_α the channel radius, and C_α and ϵ_α the Coulomb barrier and center-of-mass energy available in channel α, respectively. At low excitation energies (0 – 10 MeV) the heavy-ion channels ($\alpha + ^{22}$Na, ^{6}Li + ^{20}Ne, ^{16}O + ^{10}B, ^{12}C + ^{14}N) can carry away a substantially greater amount of angular momentum than the p and d channels, meaning that at these excitation energies the contribution of the heavy-ion channels is the most important. However, at higher excitation energies in the residual nuclei many of these channels are beginning to close and the competition will be only between the α, d, p, and n channels. Keeping these criteria in mind, we include in the

Hauser-Feshbach calculation up to 10 exit channels, and these are represented by the arrows pointing out of the compound system in Fig. 8. Hauser-Feshbach calculations were performed with the computer code HELGA[31] expanded to allow calculations with many partial waves, large radii, and up to 10 reaction channels.

The total and differential Hauser-Feshbach cross sections are of the form:

$$\sigma_{\alpha, \alpha'} = \pi \lambdabar^2 \sum_{J\pi} \frac{2J+1}{(2I+1)(2i+1)}$$

$$\times \frac{\sum_{sl} T^J_{\alpha sl} \sum_{s'l'} T^J_{\alpha's'l'}}{G(J)} , \qquad (5)$$

$$\frac{d\sigma_{\alpha, \alpha'}(\theta)}{d\Omega} = \frac{\lambdabar^2}{4} \sum_{J\pi} \frac{1}{(2I+1)(2i+1)}$$

$$\times \frac{\sum_{sl} T^J_{\alpha sl} \sum_{s'l'} T^J_{\alpha's'l'} A^{(\theta)}_J (ls l's' | J)}{G(J)} , \qquad (6)$$

where unprimed and primed quantities refer to the entrance and exit channels, respectively. Each channel α' has orbital angular momentum l' and channel spin $s' = I' + i'$ leading to a total angular momentum J. The spins I' and i' of the two reaction products are denoted by I and i in the entrance channel. The optical-model transmission coefficients $T^J_{\alpha sl}$ were calculated without any spin dependence. The angular coefficients $A_J(\theta)$ have the

form:

$$A_J(\theta)(lsl's'|J) = \sum_L P_L(\cos\theta)(2J+1)^2(2l+1)(2l'+1)(-)^{s'-s}(l0l0|L0)(l'0l'0|L0)W(llJJ;Ls)W(l'l'JJ;Ls'), \quad (7)$$

in terms of Clebsch-Gordan and Racah coefficients with $P_L(\cos\theta)$ being the Legendre polynomial.

The denominator $G(J)$ of Eqs. (4) and (5) includes all decay modes energetically open to the compound nucleus and has the form

$$G(J) = \sum_{\alpha''l''s''}\left[\sum_{E_x=0}^{E_c} T^J_{\alpha''l''s''} + \sum_{l''\pi''}\int_{E_c}^{E_{max}}\rho(\epsilon,I'',\pi'')T^J_{\alpha''l''s''}d\epsilon\right], \quad (8)$$

where the double primes refer to all possible exit channels. The sum from $E_x = 0$ to E_c is over discrete states, and the integral is calculated for continuum states derived from the level density $\rho(\epsilon,I,\pi)$ at the energy ϵ. The quantity E_{max} represents the maximum excitation energy allowed by kinematics. The level-density formula used for states of a given parity was of the form[31]

$$\rho(\epsilon,I,\pi) = \tfrac{1}{2}\omega(\epsilon)\rho(\epsilon,I),$$

where

$$\rho(\epsilon,I) = e^{-I^2/2ct} - e^{-(I+1)^2/2ct}$$

and

$$\omega(\epsilon) = \frac{e^{2(aU)^{1/2}}}{12(2ac)^{1/2}at^3}. \quad (9)$$

The parameter U can be written as $U = \epsilon - \Delta$ and $U = at^2$ where Δ and t are the pairing energy correction and nuclear temperature, respectively.
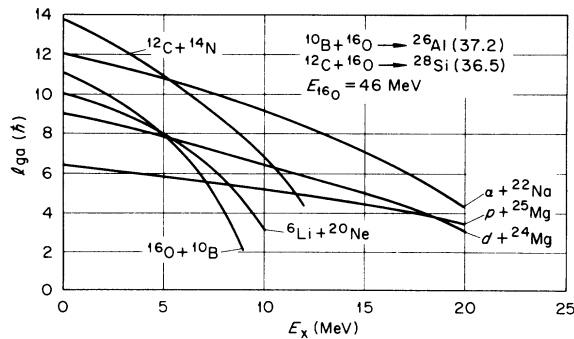

FIG. 9. A plot of the semiclassical grazing angular momentum calculated from Eq. (4) of the text for some of the more important channels included in the Hauser-Feshbach calculations.

The above form of the level-density formula reduces to the more familiar equation depending on a single exponential when $2ct \gg 1$. The parameter c is related to the spin cutoff parameter by the expression $\sigma^2 = ct$ and to the level-density parameter a by $c = (1.44/\pi^2)A^{2/3}a$.
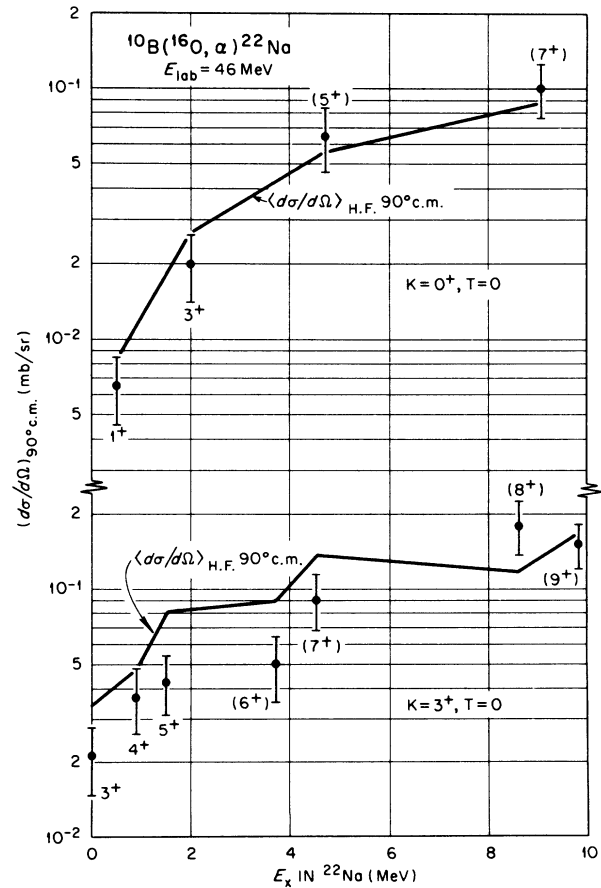
In order to compare the data with Hauser-Feshbach calculations it is necessary to find appropriate values for the level-density parameter a and pairing energy correction Δ, as well as for the optical-model parameters. The parameters used in the calculations for the ^{16}O + ^{10}B reactions are listed in Table II. The pairing energy correction Δ is taken from the work of Gilbert and Cameron,[34] and the values of a for ^{24}Mg and ^{23}Na are those obtained from (p,γ) resonances as discussed in Ref. 38. Experimental determinations of a for the nuclei ^{22}Na, ^{25}Al, and ^{25}Mg are not available and the values listed in Table II correspond to a value of $a \approx A/7.8$, consistent with the extrapolated values of $A/7.5$ (Ref. 32) or $A/8$ (Ref. 33).

Since we are interested in calculating the Hauser-Feshbach cross sections for highly excited states in ^{22}Na, and since spin and parity values are only well established for states below 6 MeV of excitation in ^{22}Na,[10-16] we used in the region from 6 to 10 MeV the excitation energies and J^π values (wherever possible) from Refs. 12–14, and from 10.0 to 13.8 MeV the states observed in the present experiment. In order to include in the Hauser-Feshbach calculations states with undetermined spin, the excitation energies for the $T = 0$ positive-parity states predicted by extensive shell-model calculations[19] were matched to our measured excitation energies. In addition, the known negative-parity bands[13] were extrapolated up to high-spin states by assuming a $J(J+1)$ dependence on the excitation energy.

With the parameters of Table II, angular distributions for the states observed in ^{22}Na were calculated with Hauser-Feshbach theory. Figure 4 shows the Hauser-Feshbach predictions (solid lines) compared to the experimental data measured at an incident energy of 17.7 MeV (c.m.). The left side of the figure displays the known and suggested members of the ground-state rotational band, and on the right side the members of the $K = 0^+$, $T = 0$ band are shown together with other states prominently excited. The angular distributions seen in Fig. 4 for the well-established 3^+, 1^+, 4^+, and 3^+ states at 0.0, 0.58, 0.89, and 1.98 MeV, respec-

TABLE II. Level-density and optical-model parameters for the ^{16}O + ^{10}B reactions.

	^{22}Na + α	^{24}Mg + d	^{25}Al + n	^{25}Mg + p	^{23}Na + ^{3}He	^{20}Ne + ^{6}Li	^{21}Ne + ^{5}Li	^{18}F + ^{8}Be	^{14}N + ^{12}C	^{10}B + ^{16}O
a [d]	2.83[a]	3.58[b]	3.1[a]	3.1[a]	3.84[b]		3.41[c]			
Δ [d]	0.0	5.13	2.67	2.46	2.67		2.25			
E_c (MeV)	13.8	16.7	8.0	6.0	5.8	12.8	3.5	10.5	11.6	10.0
No. of discrete levels	115	98	21	12	13	55	3	70	35	25
V (MeV)	99.9[e]	$89.3 - 0.22E$[f]	$47.01 - 0.26E$[f]	$53.3 - 0.55E$[f]	153.5[g]	$7.5 + 0.4E_{c.m.}$[h]				
$R_0 = r_0 A^{1/3}$ (fm)	4.19[e]	3.32[f]	3.8[f]	3.65[f]	3.27[g]	$1.35\,(A_1^{1/3} + A_2^{1/3})$[h]				
a_0 (fm)	0.6[e]	0.81[f]	0.66[f]	0.65[f]	0.69[g]	0.45[h]				
W (MeV)	11.3[e]	$14.4 + 0.24E$[f]	$9.52 - 0.05E$[f]	13.5[f]	30.5[g]	$0.4 + 0.125E_{c.m.}$[h]				
$R_i = r_i A^{1/3}$ (fm)	4.19[e]	3.86[f]	3.68[f]	3.65[f]	4.13[g]	$1.35\,(A_1^{1/3} + A_2^{1/3})$[h]				
a_i (fm)	0.60[e]	0.68[f]	0.48[f]	0.47[f]	0.89[g]	0.45[h]				
R_{Coulomb} (fm)	4.19[e]	3.32[f]		3.65	3.27[g]	$1.35\,(A_1^{1/3} + A_2^{1/3})$[h]				

[a] Values of a obtained from $a \sim A/7.8$ (see text).
[b] Values from Ref. 32.
[c] Values from Ref. 33.
[d] Values from Ref. 34.

[e] Optical-model potential from Ref. 35.
[f] Optical-model potential from Ref. 36.
[g] Optical-model potential from Ref. 37.
[h] Optical-model potential from Ref. 8 and reference cited therein.

tively, were primarily those used to determine appropriate values of the optical-model and level-density parameters involved. These values, which are in good agreement with those obtained from systematics in this mass region, at the same time gave good fits to the other angular distributions seen in Fig. 4 with the exception of those for the 5⁺ and 6⁺ states of the ground-state band. Fitting the angular distributions for these two levels would require unreasonable values for the level-density parameters and would also destroy the agreement with the other levels. However, considering that our experimental angular distributions are not averaged over bombarding energy, the Hauser-Feshbach calculations are in excellent agreement with the data. The largest deviations are for the 1.53-MeV (5⁺) and 3.71-MeV (6⁺) members of the ground-state rotational band which are overpredicted by a factor of 2. Although this discrepancy could result from fluctuation effects, it remains

FIG. 10. A comparison between the measured differential cross sections at 90° (c.m.) and the Hauser-Feshbach predictions for the known and suggested members of the $K = 3^+$ and $K = 0^+$ bands. The solid lines join the Hauser-Feshbach predictions.

even when comparing the average experimental differential cross sections with the Hauser-Feshbach predictions as will be discussed later.

The fact that the non-energy-averaged angular distributions are in good agreement with the Hauser-Feshbach calculations may be a consequence of the strong damping of the fluctuations due to the entrance channel spin $s = 3$. The excitation functions in Fig. 2 fluctuate about the average value by $\pm 40\%$ to 80%, in sharp contrast with what one sees for the ^{12}C(^{16}O, α) reaction where the fluctuations are an order of magnitude larger.[8,18] Since the number of effective channels is largest at 90° (c.m.), better agreement between the data and the Hauser-Feshbach calculations is expected at this angle due to damping of the fluctuations. Figure 10 displays this 90° comparison for some members of the $K = 3^+$ and $K = 0^+$ bands. The solid lines join the Hauser-Feshbach predictions, and there is generally good agreement with the measured cross sections.

Another interesting point apparent from Fig. 4 is that the states at 8.6 MeV (8^+), 9.86 MeV (9^+), 9.03 MeV (7^+), 9.31 MeV (7^+), 12.62 MeV (9^+), and 13.58 MeV (10^+) are high-spin states, and that the spin values suggested here result in calculated cross sections in reasonable agreement with the measured values. In order to propose candidates for the high-spin states in ^{22}Na we compared our average differential cross sections (obtained at 7° lab and from 40- to 46-MeV bombarding energy)

with the Hauser-Feshbach predictions at the approximately equivalent center-of-mass angle and energy of 10° and 17.7 MeV. The results of such a comparison are shown in Fig. 11. The histograms represent the various measured differential cross sections, and the dots are the Hauser-Feshbach predictions. Also drawn on the figure are lines showing the general change in intensity predicted by Hauser-Feshbach theory for given spin values as a function of the excitation energy. As can be seen states with spins less than 5^+ are expected to have negligible cross sections above 10 MeV. In order to locate candidates for the various high-spin states we used this intensity dependence on spin, together with the extensive shell-model calculations of McGrory.[19] The shell-model predictions are in very good agreement with the energies of the established 3^+ through 5^+ members of the ground-state rotational band. Measurements with the ^{12}C(^{14}N, α) reaction have suggested the locations of the 6^+ and 7^+ members of the ground-state band at 3.708 and 4.522 MeV,[15,16] respectively, the 8^+ member of the ground-state band at 8.60 MeV,[15] and the 5^+ member of the $K = 0^+$ band at 4.708 MeV.[15,16] Comparing our experimental spectra with the shell-model predictions,[19] we generally find only one state close to the expected energy of each band member with a strength consistent with that predicted by the Hauser-Feshbach theory. However, the Hauser-Feshbach calculations do overpredict the cross sections near 7° for
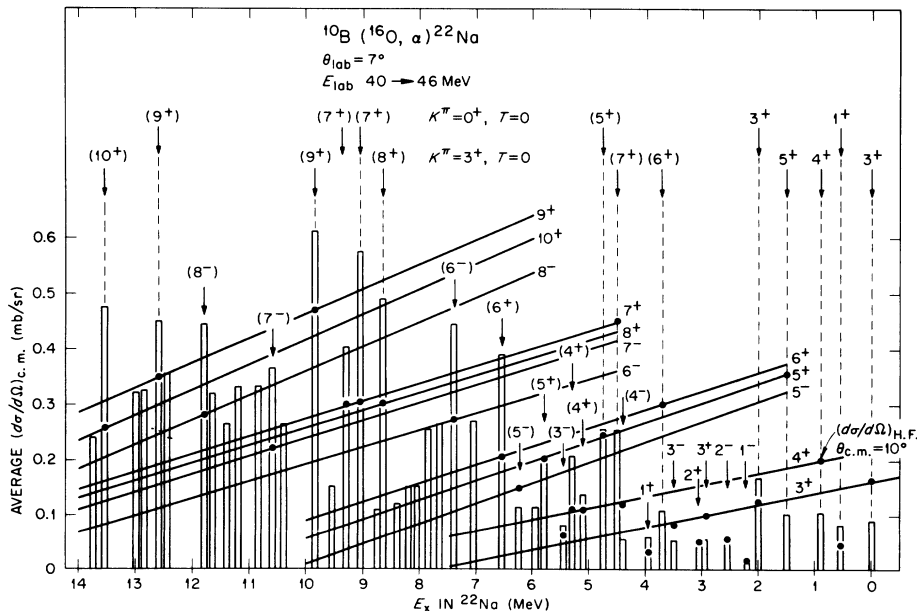

FIG. 11. A histogram representing the measured differential cross sections averaged over 40–46 MeV at 10° (c.m.). The dots are the Hauser-Feshbach predictions, and the various spins and parities of the states are discussed in the text. The straight lines indicate the general trend of the Hauser-Feshbach predictions with excitation energy for different spin values.

the 5$^+$ and 6$^+$ ground-state band members by a factor of about 3, and the 3$^+$, 4$^+$, and 7$^+$ members by about a factor of 2, although the agreement for all these states at 90° is within a factor of 2.

The first 8$^+$ state is predicted by the shell model[19] to have an excitation energy of 8.15 MeV, and as can be seen from Fig. 11 the closest state with the necessary strength is the one at 8.6 MeV. Assuming a spin of 8$^+$ for this state the Hauser-Feshbach calculations account for 67% of the observed cross section, and thus the present measurements are consistent with the 8$^+$ suggestion of Hallock *et al.*[15] for this level.

The first 9$^+$ state is predicted to be at 10 MeV by the shell-model calculations,[19] and here the situation is even less ambiguous since the only state with the required intensity in a region of $\pm\frac{1}{2}$ MeV of the predicted energy is the one at 9.86 MeV. In this case the Hauser-Feshbach calculations account for 75% of the observed strength. Also notice that the largest observed cross section is for this level in agreement with the Hauser-Feshbach prediction. Comparing the average observed cross section at 7° with the Hauser-Feshbach predictions also would permit spin values of 9$^-$ or 10$^+$ for this state. However, the angular-distribution data of Fig. 4 clearly favor a spin of 9$^+$. The experimental data are consistent with the increase in yield for angles less than 20° predicted for a 9$^+$ state; in contrast, the angular distributions for 9$^-$ or 10$^+$ states turn over at 20°. This difference in the behavior of natural- and unnatural-parity states from that normally expected is due to the entrance channel of 3$^+$ which is itself of unnatural parity.

The first 10$^+$ state is predicted to lie at an energy of 13.41 MeV, and we selected the state at 13.58 MeV as the best candidate for this level. The Hauser-Feshbach calculation is within 55% of the observed strength. State with lower spins would give still poorer agreement with the observed cross section. Assuming a spin larger than 10 would be in strong disagreement with the shell-model calculations as the first 11$^+$ state is predicted at 19.72 MeV.[19]

For the $K = 0^+$, $T = 0$ band, McGrory's calculations underpredicted the excitation energies of the 1$^+$ to 5$^+$ members by 200 keV. However, the Hauser-Feshbach calculations are in excellent agreement with the measured cross sections for these states. The second 7$^+$ state is predicted to be at 8.47 MeV with a third at 8.91 MeV. The calculated and observed cross sections suggest that these two states are the levels observed at 9.03 and 9.31 MeV, and the lower-lying level was assumed to be the candidate for the 7$^+$ member of the $K = 0^+$ band. With these assumptions, the Hauser-Feshbach calculations account for 62% of

the observed strength of the 9.03-MeV level and for 75% of that for the 9.31-MeV level. A second 9$^+$ state is predicted at an energy of 13.09 MeV, and the observed state at 12.62 MeV is the best candidate for this level. Here the Hauser-Feshbach prediction accounts for 77% of the observed strength. Here again, if the level at 12.46 MeV is instead assumed to be this 9$^+$ state, then the strength of the 12.62-MeV level requires that it have higher spin which conflicts with the shell-model predictions.

This same procedure was used to locate other predicted positive-parity states.[19] An example is shown for the states at 5.117 MeV (4$^+$) and 5.83 MeV (5$^+$) which do not have known spins. With these two exceptions, the spins below 6 MeV in excitation energy are known from Refs. 10–15.

The known 1$^-$, 2$^-$, and 3$^-$ members of the $K = 1^-$, $T = 0$ band have measured cross sections in very good agreement with the Hauser-Feshbach calculations. The suggested (4$^-$) (Refs. 15 and 16) state at 4.466 MeV has a measured cross section a factor of 2 smaller than that calculated, but in this case the experimental uncertainty is large since it was at times difficult to separate the 4.466- and 4.522-MeV levels. In order to follow the rest of the members of the $K = 1^-$ band we assumed a $J(J+1)$ energy dependence separately for the even or odd members of the band. The suggested band members are then: 6.25 MeV (5$^-$), 7.41 MeV (6$^-$), 10.61 MeV (7$^-$), and 11.82 MeV (8$^-$). Also shown in Fig. 11 are the Hauser-Feshbach predictions with these assumptions. However, the situation is more ambiguous for this band and probably other equally good candidates could be selected, particularly for the 7$^-$ and 8$^-$ members.

As can be seen from Fig. 11 there are many strong states which do not fit into any of the discussed rotational bands. Of particular interest is the state at 6.58 MeV. In an energy region within ± 50 keV of this state there is only one other known level in ^{22}Na, that at 6.55 MeV (1$^+$, 2$^+$) which according to the Hauser-Feshbach calculations should have a very small yield. The shell-model calculations predict a close-lying second 6$^+$ state at 6.8 MeV. If the state at 6.58 MeV is the expected 6$^+$ level, then the Hauser-Feshbach predictions account for 50% of the observed strength. On the other hand, the Hauser-Feshbach calculated cross section is much larger than that observed for the (6$^+$) state at 3.708 MeV. Another interesting discrepancy between the calculated and observed cross sections appears for the two lowest 5$^+$ states at 1.528 and 4.708 MeV which are populated with intensities opposite to that predicted by the Hauser-Feshbach calculations (see Fig. 11). This discrepancy does not appear to be due to a direct compo-
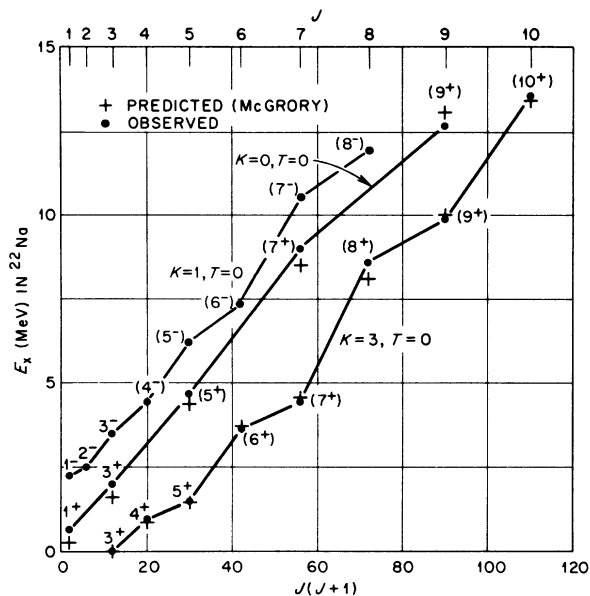
FIG. 12. A plot of the $K=3^+$, $T=0$; $K=0^+$, $T=0$; and $K=1^-$, $T=0$ rotational bands in ^{22}Na. The dots represent the experimentally observed states and the crosses are the result of the extensive shell-model calculations of McGrory (Ref. 19).

nent in the reaction mechanism, unless one assumes an improbable destructive interference between the direct and compound contributions, since the calculated cross sections for the first 5^+ and 6^+ states are larger than the observed values. Although we are comparing the calculations with average cross sections measured at a single angle and the uncertainties due to such a comparison might explain some discrepancies, the over-all good agreement between the theoretical and experimental cross sections for the members of the $K=3^+$ and $K=0^+$ bands suggests that the discrepancies for the 5^+ and 6^+ states of the $K=3^+$ band are significant. However, we do not have a sufficient explanation for them.

In Fig. 12 are summarized our results for the $K=3^+$, $T=0$ and $K=0^+$, $T=0$ bands. The dots are the experimental observations, and the crosses indicate the results of the shell-model calculations. The extrapolated candidates for the members of the $K=1^-$ band are also shown.

VI. CONCLUSION

The fluctuation analyses and symmetric angular distributions suggest that the ^{10}B(^{16}O, α)^{22}Na reaction is proceeding mainly by a statistical compound-nuclear process. The coherence widths for the compound-nucleus states derived from the fluctuation analyses are also in reasonable agreement with systematics for the mass and region of excitation energy involved.

The Hauser-Feshbach calculations are in general agreement with most of the data and suggest that such calculations are a useful means to select high-spin states excited in heavy-ion reactions. Comparing our spectra with such calculations, we suggest strong candidates for members of the $K=3^+$, $T=0$ and $K=0^+$, $T=0$ rotational bands up through the 10^+ and 9^+ members, respectively. Members of the $K=1^-$, $T=0$ band up through the 8^- state are also suggested.

*Instituto de Fisica, Universidad Nacional Autonoma de Mexico, Mexico 20, D. F. Supported in part by Instituto Nacional de Energia Nuclear, Mexico.

†Operated by Union Carbide Corporation for the U. S. Atomic Energy Commission.

‡Research participation at Oak Ridge National Laboratory sponsored in part by Oak Ridge Associated Universities.

[1] R. Middleton, J. D. Garrett, and H. T. Fortune, Phys. Rev. Lett. 24, 1436 (1970).

[2] A. Gobbi, P. R. Maurenzig, L. Chua, R. Hadsell, P. D. Parker, M. W. Sachs, D. Shapira, R. Stokstad, R. Wieland, and D. A. Bromley, Phys. Rev. Lett. 26,

396 (1971).

[3] R. Middleton, J. D. Garrett, and H. T. Fortune, Phys. Rev. Lett. 27, 950 (1971).

[4] M. L. Halbert, F. E. Durham, and A. van der Woude, Phys. Rev. 162, 899 (1967).

[5] M. L. Halbert, F. E. Durham, C. D. Moak, and A. Zucker, Phys. Rev. 162, 919 (1967).

[6] E. Almqvist, J. A. Kuehner, D. McPherson, and E. W. Vogt, Phys. Rev. 136, B84 (1964).

[7] R. W. Shaw, J. C. Norman, R. Vandenbosch, and C. J. Bishop, Phys. Rev. 184, 1040 (1969).

[8] L. R. Greenwood, K. Katori, R. E. Malmin, T. H. Braid, J. C. Stoltzfus, and R. H. Siemssen, Phys. Rev.

C 6, 2112 (1972).

[9]R. Stokstad, cited by R. Middleton, in *Proceedings of Heavy-Ion Summer Study, CONF-720669, Oak Ridge National Laboratory, June, 1972,* edited by S. T. Thornton (National Technical Information Services, U. S. Department of Commerce, Springfield, Va., 1972), p. 315.

[10]E. K. Warburton, A. R. Poletti, and J. W. Olness, Phys. Rev. 168, 1232 (1968); J. W. Olness, W. R. Harris, P. Paul, and E. K. Warburton, Phys. Rev. C 1, 958 (1970).

[11]K. W. Jones, A. Z. Schwarzschild, E. K. Warburton, and D. B. Fossan, Phys. Rev. 178, 1773 (1969).

[12]J. D. Garrett, R. Middleton, and H. T. Fortune, Phys. Rev. C 4, 165 (1971).

[13]J. D. Garrett, H. T. Fortune, and R. Middleton, Phys. Rev. C 4, 1138 (1971).

[14]J. D. Garrett, R. Middleton, D. J. Pullen, S. A. Anderson, O. Nathan, and O. Hansen, Nucl. Phys. A164, 449 (1971).

[15]J. N. Hallock, H. A. Enge, A. Sperduto, R. Middleton, J. D. Garrett, and H. T. Fortune, Phys. Rev. C 6, 2148 (1972).

[16]M. J. Schneider and J. W. Olness, Bull. Am. Phys. Soc. 17, 528 (1972); and private communication.

[17]J. L'Ecuyer, N. Marquardt, C. Cardinal, J. M. Poutissou, R. Volders, Université de Montréal Rapport d'Activité No. 73, 1972 (unpublished).

[18]J. L. C. Ford, Jr., J. Gomez del Campo, R. L. Robinson, P. H. Stelson, and S. T. Thornton, to be published.

[19]J. B. McGrory, private communication.

[20]C. J. Borkowski and M. K. Kopp, IEEE Trans. Nucl. Sci. 17, No. 3, 340 (1970).

[21]J. L. C. Ford, Jr., P. H. Stelson, and R. L. Robinson, Nucl. Instrum. Methods 98, 199 (1972).

[22]T. D. Thomas, Ann. Phys. (N. Y.) 23, 390 (1963).

[23]T. Ericson, Phys. Rev. Lett. 5, 430 (1960); Ann. Phys. (N. Y.) 23, 390 (1963).

[24]D. M. Brink and R. O. Stephen, Phys. Lett. 5, 77 (1963).

[25]H. A. Weidenmüller, unpublished lecture notes.

[26]W. R. Gibbs, in *Proceedings of the International Conference on Statistical Properties of Nuclei,* edited by J. B. Garg (Plenum, New York, 1972), p. 131.

[27]K. A. Eberhard and A. Richter, in *Proceedings of the International Conference on Statistical Properties of Nuclei* (see Ref. 26), p. 139.

[28]P. G. Bizzeti and P. R. Maurenzig, Nuovo Cimento 47B, 29 (1967).

[29]P. A. Moldauer, Phys. Rev. Lett. 18, 249 (1967).

[30]M. Böhning, in *Nuclear Reactions Induced by Heavy Ions,* edited by R. Bock and W. R. Hering (North-Holland, Amsterdam, 1970), p. 633.

[31]S. K. Penny, Oak Ridge National Laboratory, private communication.

[32]W. R. Falk, A. Huber, V. Matter, R. W. Benjamin, and P. Marmier, Nucl. Phys. A140, 548 (1970).

[33]D. W. Lang, Nucl. Phys. 77, 545 (1966).

[34]A. Gilbert and A. G. W. Cameron, Can. J. Phys. 43, 1446 (1965).

[35]L. McFadden and G. R. Satchler, Nucl. Phys. 84, 177 (1966).

[36]C. M. Perey and F. G. Perey, Nucl. Data B10, 539 (1972).

[37]R. C. Bearse, Phys. Rev. 175, 1442 (1968).

[38]V. Facchini and E. Saetta-Menichella, Energ. Nucl. (Milan) 15, 54 (1968).